

JOE/BC/14990--12

BC/14990-12

**TITLE: APPLICATION OF RESERVOIR CHARACTERIZATION AND ADVANCED TECHNOLOGY TO IMPROVE RECOVERY AND ECONOMICS IN A LOWER QUALITY SHALLOW SHELF CARBONATE RESERVOIR**

Cooperative Agreement No.: DE - FC22 - 94BC14990

Contractor Name and Address: Oxy USA, Inc. (Oxy), Midland, Texas

Date of Report: September 23, 1996

Award Date: August 3, 1994

Anticipated Completion Date: December 31, 1996 - Budget Period 1

Government Award for Current Fiscal Year: \$2,023,000

Principal Investigators: Archie R. Taylor (Oxy)

Project Manager: Chandra Nautiyal, Bartlesville Project Office

Reporting Period: August 2, 1995 through August 3, 1996

RECEIVED

APR 07 1997

OSTI

DISTRIBUTION OF THIS DOCUMENT IS UNLIMITED *ph*

**MASTER**

**DISCLAIMER**

**Portions of this document may be illegible  
in electronic image products. Images are  
produced from the best available original  
document.**

## DISCLAIMER

This report was prepared as an account of work sponsored by an agency of the United States Government. Neither the United States Government nor any agency thereof, nor any of their employees, make any warranty, express or implied, or assumes any legal liability or responsibility for the accuracy, completeness, or usefulness of any information, apparatus, product, or process disclosed, or represents that its use would not infringe privately owned rights. Reference herein to any specific commercial product, process, or service by trade name, trademark, manufacturer, or otherwise does not necessarily constitute or imply its endorsement, recommendation, or favoring by the United States Government or any agency thereof. The views and opinions of authors expressed herein do not necessarily state or reflect those of the United States Government or any agency thereof.

## TABLE OF CONTENTS

Title Page .....	Page 1
Table of Contents .....	Page 2
Abstract .....	Page 3
Executive Summary .....	Page 4
Discussion .....	Page 6
Appendix A	
Figure 1 - Incremental Oil Recovery vs MCF of CO <sub>2</sub> Injected per Porosity-foot for the Producing Interval	
Figure 2 - Flow Chart for Permeability Computation	
Figure 3 - Whole Core Permeability Vs Computed Permeability	
Figure 4 - Cross Section of Welch Field	
Figure 5 - Processed Seismic Section	
Figure 6 - Reprocessed Seismic Section	
Figure 7 - Cross Well Computed Velocities vs Core Porosity	
Figure 8 - Project Area History Match	

## ABSTRACT

The Oxy West Welch project is designed to demonstrate how the use of advanced technology can improve the economics of miscible CO<sub>2</sub> injection projects in lower quality shallow shelf carbonate reservoirs. The research and design phase primarily involves advanced reservoir characterization and the demonstration phase will implement the reservoir management plan based on an optimum miscible CO<sub>2</sub> flood as designed in the initial phase.

The reservoir characterization phase is near completion with the tomography currently being integrated into the petrophysical and 3-D seismic interpretations. The petrophysical analysis has yielded both an improved net pay criteria and a method of calculating permeability from log response. The 3-D seismic has enhanced the ability to distribute the reservoir properties between wellbore control points.

During the reporting period, work was completed on the CO<sub>2</sub> stimulation treatments and the hydraulic fracture design. Analysis of the CO<sub>2</sub> stimulation treatment provided a methodology for predicting results. The hydraulic fracture treatment proved up both the fracture design approach and the use of passive seismic for mapping the fracture wing orientation.

## EXECUTIVE SUMMARY

The West Welch Unit is one of four large waterflood units in the Welch Field located in the northwestern portion of Dawson County, Texas. The Welch Field was discovered in the early 1940's and produces oil under solution gas-drive mechanism from the San Andres formation at approximately 4800 ft. The field has been under waterflood for 30 years and a significant portion has been infill drilled on 20-acre density. A 1982-86 pilot CO<sub>2</sub> injection project on the offsetting South Welch Unit yielded positive results. The recent installation of a CO<sub>2</sub> pipeline near the field allowed the phased development of a miscible CO<sub>2</sub> injection project at the South Welch Unit.

The reservoir quality is poorer at the West Welch Unit due to its relative position at sea level during deposition. Because of the proximity of the CO<sub>2</sub> source and the CO<sub>2</sub> operating experience that would be available from the South Welch Unit, West Welch is the ideal location for demonstrating methods for enhancing economics of IOR projects in lower quality shallow shelf carbonate reservoirs.

The West Welch project is divided into two phases - Budget Periods 1 and 2. Budget Period 1 involves a detailed reservoir characterization effort which integrates advanced petrophysics with 3-D seismic and tomography to identify major flow units and their inter-well distribution. The resulting geologic model will be used in a reservoir simulator which will serve as a basis for developing an optimum CO<sub>2</sub> miscible flood design. Budget Period 2 will be the installation and actual field demonstration of the project.

The bulk of the effort during the current reporting period has been devoted to continuing the reservoir characterization effort. The detailed petrophysical analysis has yielded a methodology for obtaining usable permeability values on a foot by foot basis from conventional log response. The 3-D seismic effort during the past year has focused mainly on refining the interpretation through enhanced processing and decreased bin size. Processing of the tomography data has only recently been completed. The resulting tomograms are being integrated with the petrophysical and 3-D seismic data.

Although the simulator currently contains only the basic geologic model, considerable progress has been made in matching actual performance.

The CO<sub>2</sub> stimulation treatments were analyzed and a method developed to predict future performance. The disappointing results realized from the treatments related mainly to the small volumes of CO<sub>2</sub> injected. Once pipeline CO<sub>2</sub> becomes available the process should be economical.

Data obtained from the hydraulic fracture treatment on WWU 4807 was analyzed. It was concluded that fracture treatments can be designed with reasonable accuracy if the model contains sufficient information as to reservoir layering. It was

also determined that passive seismic can be used to map the fracture wing orientation and dimensions of the fracture created, which may be substantially different than dimensions after fracture closure.

## DISCUSSION

### CO<sub>2</sub> STIMULATION TREATMENTS

All of the CO<sub>2</sub> injection occurred during the first annual reporting period, but monitoring of the test wells has continued. Evaluation of the data generated from the five well treatments has demonstrated the process can be economic with pipeline CO<sub>2</sub> in some cases. Figure 1 shows the incremental production versus the wellbore porosity feet for actual and predicted recovery. The incremental production is calculated from production above the rate prior to treatment, allowing for reduced base production while the well is actually flowing or producing with very high fluid levels. Lost or deferred production from the period the well is shut-in for injection or soaking is not included in the incremental oil calculation.

The calculation of incremental recovery uses fractional flow theory and laboratory PVT data to estimate the volume of oil affected by a treatment. An example calculation is shown in Appendix A. The treated radius is calculated using the average gas saturation from the gas/oil fractional flow curve with the total CO<sub>2</sub> volume pumped and the total pore volume in the volumetric equation. The CO<sub>2</sub> volume dissolving in water and the free gas volume is estimated to determine the CO<sub>2</sub> volume available for swelling oil. This volume determines the CO<sub>2</sub> mole fraction in the oil and the oil swelling factor. Using the oil swelling factor, the incremental oil is calculated from the difference in oil saturations before and after swelling and the residual oil saturation to waterflooding.

Based on the work to date, an estimated 40 MSTB of oil will be produced during the first year of the project by the treatment of 17 producing wells.

### HYDRAULIC FRACTURING

Initial passive seismic results from the fracture treatment on the 4807 well were not as anticipated. The initial interpretation identified 30 seismic events that have at least five clear signals from different stations. Results from the 30 events show one wing of the fracture extends over 500 feet to the east with one event occurring at 90 degrees to and 500 feet from the east end of the fracture. Propagation of the other wing appears to have gone to the southeast for over 1000 feet. However, the seismic events, at the ends of the fracture, suggest that the fracture grew out, then upward completely out of the main pay.

The falloff analysis gave more conventional results, showing an effective fracture half length of 400 feet assuming 60 feet pay thickness. This is similar to the fracture area predicted by the fracture modeling. However, the post-fracture model shows the fracture grew out of zone at the wellbore, with a fracture height of 174 feet and a half length of 180 feet.

The 3-D seismic fault maps showed that the reason the orientation was different was the presence of a deep fault running parallel to the fracture orientation observed with passive seismic. This changed the stress field in a very localized region around the fault. The change in stresses changed the orientation of the fracture as the fracture grew away from the wellbore and encountered the different stress field.

Cost estimates for Budget Period 2 fracture treatments were made using the information gained from the previous fracture treatment. The fracture treatments will be performed during the early part of Budget Period 2 with the purpose of improving injectivity and sweep improvement of the CO<sub>2</sub> flood. Preliminary simulation runs have shown the treatments will be able to accelerate and improve recovery.

### PETROPHYSICAL ANALYSIS

Detail work with the Carman Kozeny equation resulted in derivation of a permeability relationship utilizing information from standard porosity-resistivity log suites. The use of neural network analysis helped identify what log responses have meaningful relationships to the functions in the Kozeny equation. Gamma-ray log response has been found to correlate to surface area. Resistivity response has been used to derive the required cementation factor. The resulting equation is shown below:

$$\frac{100 \times \phi^3}{m_{NR} \times GR^2 \times (1 - \phi)}$$

Where,	K	=	Permeability, (md)
	$\phi$	=	porosity, fraction
	$m_{NR}$	=	Nugent cementation factor calculated from the resistivity porosity
	GR	=	Normalized Gamma Ray response in the interval (Ranges $>0 \geq 1$ ; 0 values cause division by zero)

Permeability estimation from well log data was found to require three different methods. The method is determined by use of the normalized gamma ray, deep resistivity curve and effective porosity as follows: (1) if the normalized gamma ray is less than .25 and either the deep resistivity is less than 50 ohms or the effective porosity is less than .04, then permeability is estimated from a scaled cementation exponent using the Focke and Munn<sup>1</sup> equation, (2) if the deep resistivity is less than 50 ohms or the effective porosity is less than .04, and the normalized gamma ray is greater than .25, then permeability is estimated from a scaled cementation exponent using the Nugent<sup>2</sup> equation with a resistivity-derived porosity, and (3) if the porosity is greater than .04 and the deep resistivity is greater than 50 ohms, permeability is found from a Modified Carman Kozeny<sup>3</sup> equation. A flow chart of the logic is shown in Fig. 2.

The above procedure is found to give results at least as good as the agreement between plug and whole core-derived permeabilities when applied section by section over the entire gross interval. Figure 3 compares the permeability from each method

to the whole core permeability for WWU 7916. The composite results are shown in the fourth (right) panel.

Open hole logs were used to calculate permeabilities for wells in the area. Figure 4 shows the comparison of the log, plug and whole core permeabilities where core and modern open hole logs were available for the same wells. The interval where core and log calculated permeabilities failed to match was described as oolitic in the core description. Otherwise, differences in sample interval size caused the apparent difference in core and log calculated permeabilities.

Grids of porosity and permeability values, for use in the numerical simulator, were then generated using well log and core data. Wellbore data values that were obviously too high were discarded for the initial grid generation. These discarded values were from cased-hole compensated neutron logs.

### **3-D SEISMIC INTERPRETATION**

Depth structure maps of the base of the Woodford and the Atoka horizons were generated from the 3-D seismic volume. This was used to better define the deep seated (Pennsylvanian and deeper) faulting that lies beneath the producing San Andres formation. A coherency slice map of the base of Woodford horizon was produced to help delineate the small faults in the deep section. This information aided in the hydraulic fracture orientation evaluation as discussed above.

The surface seismic data has been reprocessed to decrease the bin spacing. Advances made since the initial processing in 1992 were used to enhance the data. The result is a greatly improved seismic section with increased signal to noise ratio, more dense areal spacing and higher frequencies. Figures 5 and 6 compare the before and after sections respectively.

### **TOMOGRAPHY**

Integration of the cross well seismic velocities and wellbore data showed a distinct correlation to core porosity (Fig. 7); however, the correlation appeared limited at a maximum value. As a result, cross well velocities were modeled, using a 1-D model, to better define the time interval where the tomography event should be picked. The model resolves variations in picking arrivals from changes in source waveform due to changing source positions, and changes in receiver orientation resulting in phase and polarity changes between receiver stations.

Compressional wave and shear wave processing is complete for the 15 lines. The early results show the shear wave data give more detail than the compression wave data collected at the same sampling rates. This is due to the lower shear wave velocities which result in more accuracy in the processing.

Integration of the petrophysical and 3-D seismic data with the tomograms is currently underway.

### **RESERVOIR SIMULATION**

A preliminary history match was made for the base geologic model and the results used to make limited forecasts for screening economics. The grid is 57 x 65 x 9 layers resulting in an approximate 80 ft. grid size to minimize the numerical dispersion effects. Steady state simulations and production type curves were used to provide permeability and effective thickness multipliers for the history match. The steady state simulations matched the late waterflood history when reservoir saturations are relatively constant thus setting the permeability-thickness needed for the history match. The type curves are plots of WOR versus fraction of oil recovered to determine the net pay thickness needed to modify the reservoir description to match the historical performance. Utilizing the different relative permeabilities by rock type in the base geologic model created slight improvements in the history match.

The history match in Fig. 8 shows effective water injection was about 60-70% during most of the flood history. The model shows that most losses occurred when surface injection pressures were at 1800 psi during the late 1970s and 1980s. Since injection pressures were lowered in 1990, injection volumes are close to 100% effective. This result correlates well with the fracture gradients from the available step rate tests.

### **TECHNOLOGY TRANSFER**

During the second annual reporting period, nine presentations were made before various industry groups. In addition, four poster sessions were conducted at technical meetings. Three technical papers have been published by team members on various aspects of the project<sup>1,2,3</sup>.

Two all-day seminars were conducted at the CEED/Petroleum Industrial Alliance facility between Midland and Odessa. Five different team members made presentations concerning the engineering, petrophysics, geologic, seismic and tomographic aspects of the project. Included was a actual demonstration of the seismic attribute to log property conversion method using commercially available software on a PC.

## REFERENCES

1. Hinterlong, G. D. and Watts, G. P. et al. Seismic Estimation of Porosity in the Permian San Andres Carbonate Reservoir, Welch Field, Dawson County, Texas, Society of Independent Petroleum Earth Scientists, Dallas, TX., 20-22 March 1996.
2. Taylor, A.R., Brown, K. et al. Fracture Monitoring Using "Low Cost" Passive Seismic, *SPE 35230*, Permian Basin Oil & Gas Recovery Conference, Midland, TX 27-29 March 1996.
3. Hinterlong, G.D. and Taylor A.R. Characterization of Rock Types with Mixed Wettability using Log and Core Data - DOE Project Welch Field, Dawson County, Texas. *SPE 35160*, Permian Basin Oil & Gas Recovery Conference, Midland, TX 27-29 March 1996.

## Appendix A

### Recoverable Oil Calculation for Cyclic CO<sub>2</sub> Treatments

The reservoir CO<sub>2</sub> volume is calculated from the injection volume using the formation volume factor.

$$I_{CO_2} \times B_{g_{CO_2}} = Res. Vol_{CO_2}$$

From gas fractional flow curves, the average gas saturation behind the front is found from the tangent to the fractional flow curve, at the gas saturation at breakthrough, extrapolated to a gas fractional flow of 100%. For the West Welch project immiscible gas-oil relative permeability data shows an average saturation from fractional flow curves of 14%.

Assuming an average gas saturation over the entire completion interval, the equivalent radius of affected oil is found by

$$r_{eg} = \sqrt{\frac{Res. Vol_{CO_2} \times 5.615}{\Pi \times \phi \times H \times S_{g_{ave}}}}$$

Due to the preferential diffusion of CO<sub>2</sub> into the water phase the volume of CO<sub>2</sub> dissolving in the reservoir water is found from the solubility of CO<sub>2</sub> in water and the volume of reservoir water.

$$Vol_{gw} = \frac{\Pi \times r_{eg}^2 \times H \times \phi}{5.615} \times S_{gw}$$

The reservoir volume of free CO<sub>2</sub> remaining after the oil is saturated after soaking is estimated. From Welch cyclic CO<sub>2</sub> data the free gas volume is about 15-20% of total injection for the five wells tested.

$$Vol_{fg} = G_f \times B_g$$

The volume of CO<sub>2</sub> available to swell oil is found from the difference in the total injection and the volumes of CO<sub>2</sub> dissolved in water and free gas remaining.

$$Vol_{go} = I_{CO_2} - Vol_{gw} - Vol_{fg}$$

The volume of oil swelled depends on the radius the CO<sub>2</sub> covers  $r_{eg}$ .

$$Vol_{oil} = \frac{\Pi \times r_{eg}^2 \times H \times \phi}{5.615} \times S_o$$

The oil swelling factor is based on the mole % of CO<sub>2</sub>, therefore the moles of CO<sub>2</sub> and the moles of oil need to be calculated. The molar volume of oil is found by

$$molevol_{oil} = \frac{Mw_o}{350 \times SG_o}$$

The actual moles of oil and CO<sub>2</sub> are calculated.

$$mole_{oil} = \frac{Vol_{oil}}{molevol_o}$$

$$CO_2 mole\% = \frac{mole_{CO_2} = \frac{Vol_{go}}{mole_{CO_2} vol_g}}{mole_{CO_2} + mole_{oil}}$$

The mole% of CO2 is then

The oil swelling factor for the mole % CO2 is found from the laboratory test data. The swelling factor for Welch crude is about 1.2 for 40% CO2 in the oil. The total oil recovered from the CO2 treatment is the oil in place in the affected radius less the residual oil,

$$N_p = N \times \frac{(S_o \times S_f - S_{orw})}{(S_o \times S_p)}$$

The incremental oil is found from the difference in recovery with swelled versus unswelled oil.

$$N_{pinc} = N \times \left[ \frac{(S_o \times S_f - S_{orw})}{(S_o \times S_p)} - \frac{(S_o - S_{orw})}{S_o} \right]$$

The symbols used are

- $I_{CO_2}$  = The volume of CO2 injected in MCF
- $B_g$  = The formation volume factor RB/MCF
- $r_{eg}$  = The radius affected by CO2 injection, feet
- $H$  = Net pay interval, feet
- $\Phi$  = Average porosity over the net pay interval, fraction
- $S_{gavc}$  = Average gas saturation behind a front from fractional flow curves
- $S_{gw}$  = The solubility of CO2 in water at reservoir pressure, barrels per barrel
- $Vol_{gw}$  = The volume of CO2 dissolved in the water phase, Barrels
- $Vol_{fg}$  = The volume of free CO2 not dissolving in the oil or water, Barrels
- $G_f$  = The volume of free CO2 not dissolved in oil or water in the reservoir, MCF
- $Vol_{go}$  = The volume of CO2 dissolved in the oil, barrels
- $Vol_{oil}$  = The volume of oil affected by the CO2 injection, barrels
- $S_o$  = The current oil saturation, fraction
- $molevol_o$  = The barrels of oil in one mole of unswelled oil
- $Mw_o$  = The molecular weight of the oil, lbs/mole
- $SG_o$  = The oil specific gravity,
- $mole_o$  = The moles of oil affected by CO2
- $mole_{CO_2}$  = The moles of CO2 dissolved in the oil
- $Vol_g$  = The reservoir volume of CO2 per mole of CO2, barrels/mole
- $S_f$  = The swelling factor of the reservoir oil at the mole% of CO2
- $S_{orw}$  = The residual oil saturation to water flooding, fraction
- $N$  = The current oil in place based on the calculated radius of oil affected by CO2, STB
- $N_p$  = The total production during the stimulation period, STB
- $N_{pinc}$  = The incremental oil production from the stimulation treatment, STB

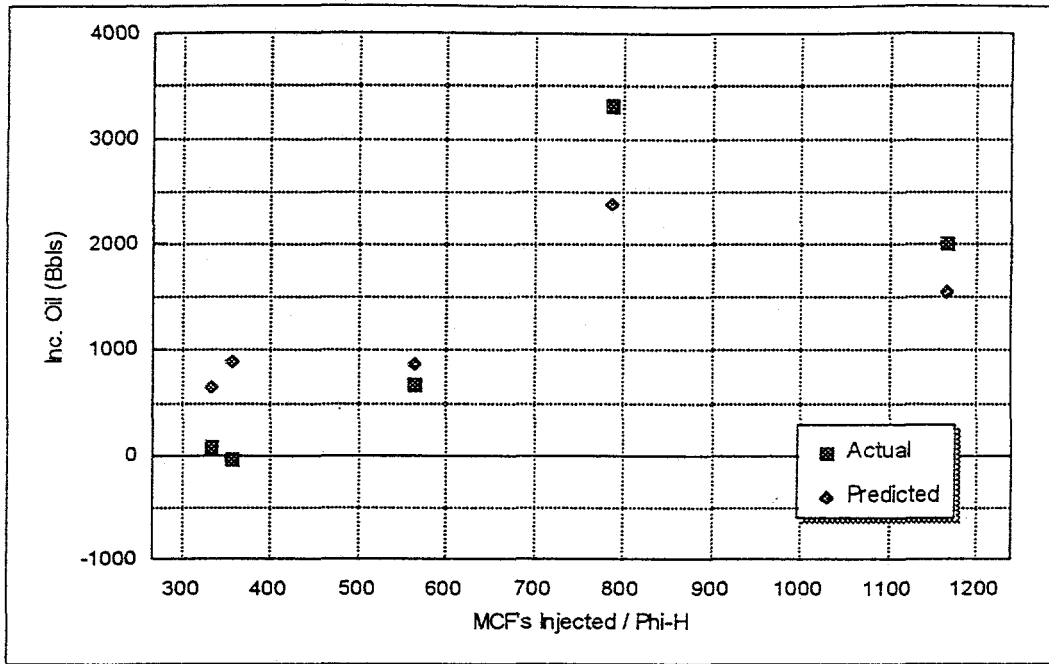


**Figure 1** Incremental oil recovery versus MCF of CO2 injected per porosity foot.

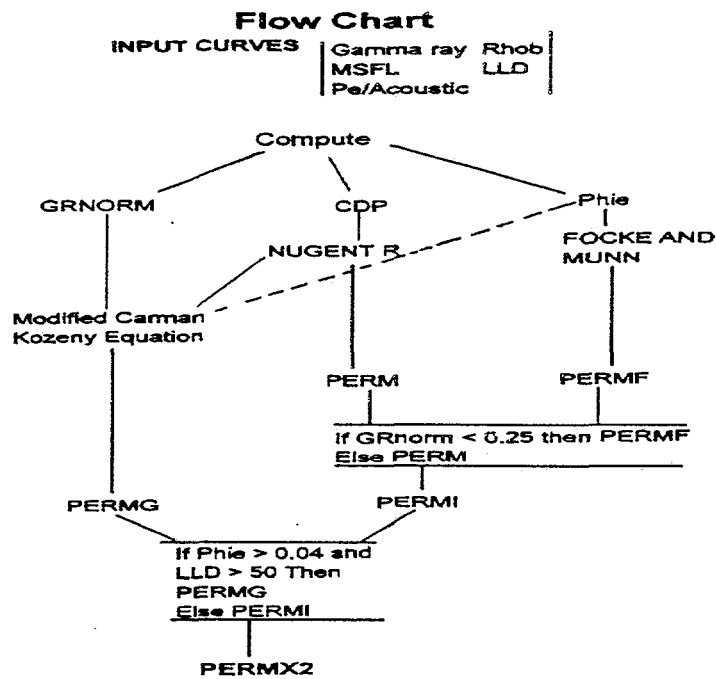


**Figure 2** Flow chart of permeability computation from log data.



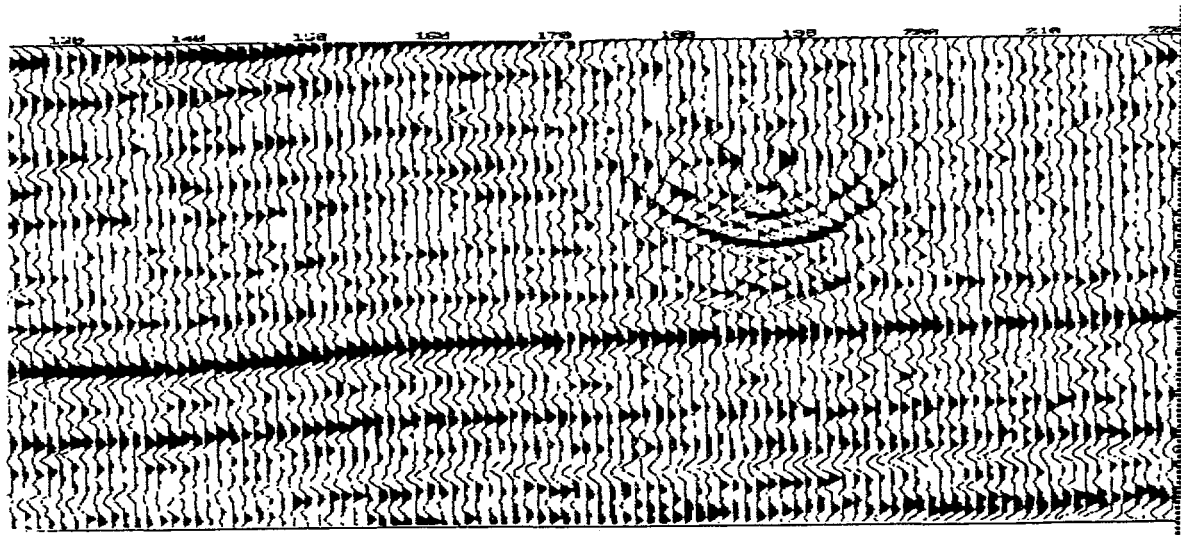


Figure 5 1992 processed seismic section.

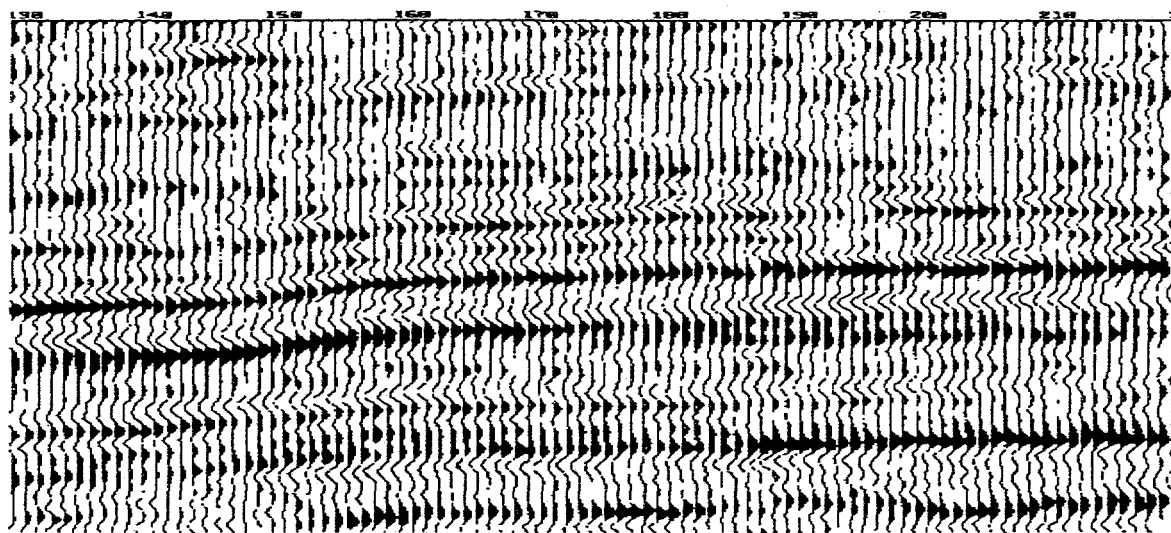


Figure 6 Current processing seismic section with smaller bin spacing.

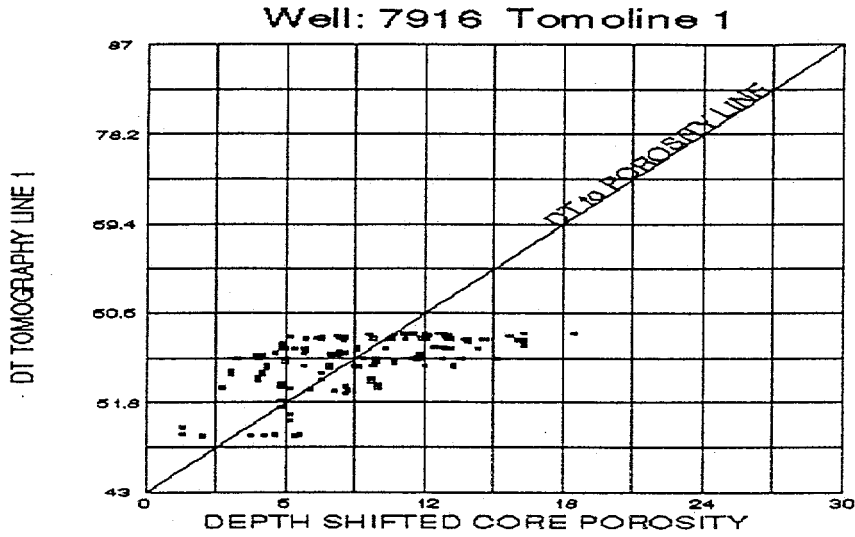


Figure 7 Computed crosswell velocities versus core porosity.

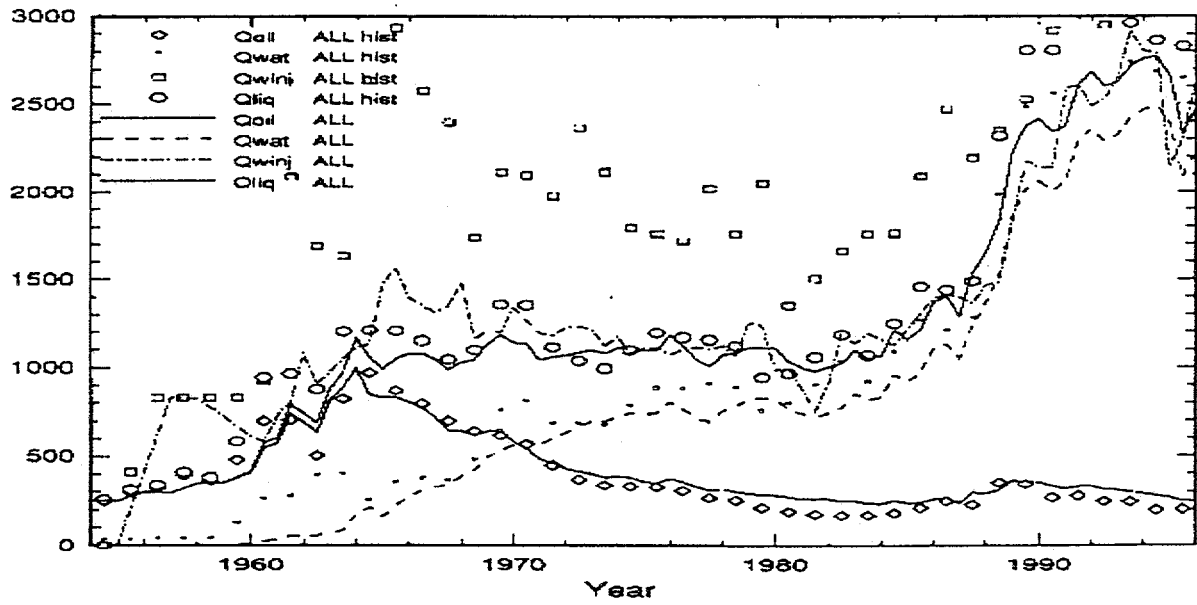


Figure 8 Comparison of model and historical production.